The MSSM golden region and its collider signature

Maxim Perelstein and Christian Spethmann

Cornell Institute for High-Energy Phenomenology, Cornell University, Ithaca, NY 14853

Abstract. The "golden region" in the Minimal Supersymmetric Model (MSSM) parameter space is the region where the experimental constraints are satisfied and the amount of fine-tuning is minimized. In this region, the stop trilinear soft term A_t is large, leading to a significant mass splitting between the two stop mass eigenstates. As a result, the decay $\tilde{t}_2 \to \tilde{t}_1 Z$ is kinematically allowed throughout the golden region. We propose that the experiments at the Large Hadron Collider (LHC) can search for this decay through an inclusive signature, $Z + 2j_b + \not{E}_T + X$. We evaluate the Standard Model backgrounds for this channel, and identify a set of cuts that would allow detection of the supersymmetric contribution at the LHC for the MSSM parameters typical of the golden region.

PACS. 14.80.Ly Supersymmetric partners of known particles – 12.60.Jv Supersymmetric models

1 The MSSM Golden Region

In this talk (based on our recent paper [1]) we explore the idea that data and naturalness point to a particular "golden" region within the Higgs and top sectors of the minimal supersymmetric model (MSSM), where the experimental bounds from non-observation of superpartners and the Higgs boson are satisfied and fine-tuning is close to the minimum value possible.

We start by outlining the boundaries of the MSSM golden region. These are somewhat fuzzy due to an inherent lack of precision surrounding the concept of fine-tuning. Our goal is to understand the qualitative features by making approximations which greatly clarify the picture.

The Higgs sector of the MSSM is strongly coupled to the top sector, but couplings to the rest of the MSSM are weaker. One may therefore begin by considering the Higgs and top sectors in isolation; that is, the gauge and non-top Yukawa couplings are set to zero. This is a good approximation as long as $M_1/M_{\tilde{t}} \lesssim 4$, $M_2/M_{\tilde{t}} \lesssim 2$, $M_3/M_{\tilde{t}} \lesssim 10, M_{\tilde{b}} \lesssim 35 M_{\tilde{t}}/\tan\beta$, where $g_{1,2,3}$ and $M_{1,2,3}$ are the gauge couplings and (weak-scale) gaugino masses for $U(1)$, $SU(2)$ and $SU(3)$, and $M_{\tilde{t}}$ and $M_{\tilde{b}}$ are the stop and sbottom mass scales. In this approximation, physics is described in terms of the holomorphic Higgs mass μ and the six parameters appearing in the soft Lagrangian for the Higgs and top sectors. Since the model has to reproduce the known EWSB scale, $v = 174$ GeV, only six parameters are independent. We choose the physical basis:

$$\tan\beta, \mu, m_A, \tilde{m}_1, \tilde{m}_2, \theta_t, \tag{1}$$

where m_A is the CP-odd Higgs mass, $\tilde{m}_1$ and $\tilde{m}_2$ are stop eigenmasses (by convention, $\tilde{m}_2 > \tilde{m}_1$) and θ_t is the stop mixing angle. We will analyze the fine-tuning and Higgs mass constraints in this approximation and map out the golden region in the six-parameter space (1).

Following Barbieri and Guidice [2], we quantify fine-tuning by computing

$$A(\xi) = \left| \frac{\partial \log m_Z^2}{\partial \log \xi} \right|, \tag{2}$$

where m_Z is the tree-level Z mass in the MSSM and $\xi = m_u^2, m_d^2, b, \mu$ are the relevant Lagrangian parameters. The overall fine-tuning Δ is defined by adding the four A's in quadruture. For concreteness, we will require $\Delta \leq 100$, corresponding to fine tuning of 1% or better. This requirement maps out the golden region in the space of $(\tan\beta, \mu, M_A)$, as illustrated in figure 1.

The largest one-loop quantum correction to the Z mass in the MSSM is due to the contribution to $\delta m_{H_u}^2$ from top and stop loops:

$$\delta_t m_Z^2 \approx -\delta m_{H_u}^2 \left(1 - \frac{1}{\cos 2\beta}\right), \tag{3}$$

where we ignored the renormalization of the angle β by top/stop loops (the contribution of this effect scales as $1/\tan^2\beta$ and is subdominant for $\tan\beta \gtrsim 2$). To measure the fine-tuning between the bare (tree-level) and one-loop contributions, we introduce

$$\Delta_t = \left| \frac{\delta_t m_Z^2}{m_Z^2} \right|. \tag{4}$$

Choosing the maximum allowed value of Δ_t selects a region in the stop sector parameter space, $(\tilde{m}_1, \tilde{m}_2, \theta_t)$, whose shape is approximately independent of the other parameters. This constraint is shown by the black (dashed) lines in Figs. 2, where we plot 5%, 3%, 1%

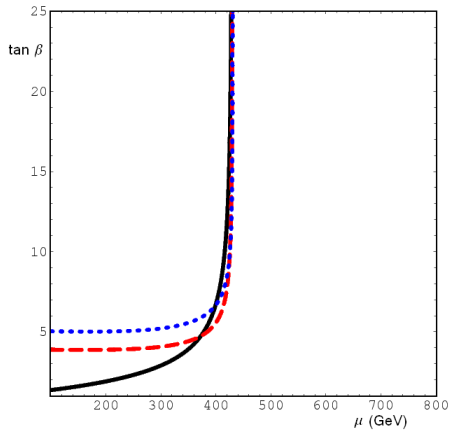

Fig. 1. Contours of 1% fine-tuning in the $(\mu, \tan\beta)$ plane. The black (solid) contour corresponds to $m_A = 100$ GeV, the red (dashed) and blue (dotted) contours correspond to $m_A = 1.5$ and 2 TeV, respectively.

and 0.5% tuning contours (corresponding to $\Delta_t = 20, 33.3, 100$, and 200, respectively) in the stop mass plane for several values of θ_t and $\tan\beta = 10$.

The second constraint that determines the shape of the golden region is the LEP2 lower bound on the Higgs mass [3]. For generic MSSM parameter values, the limit on the lightest CP-even Higgs is very close to that for the SM Higgs, $m(h^0) \gtrsim 114$ GeV, and large loop corrections are required to satisfy this bound. We used a simple analytic approximation, due to Carena *et. al.* [7], which includes the one-loop and leading-log two-loop contributions from top and stop loops. It agrees with the state-of-the-art calculations to within a few GeV for typical MSSM parameters [5].

The contours in the stop mass plane corresponding to the LEP2 Higgs mass bound are superimposed on the fine-tuning contours in Figs. 2. The positions of these contours depend strongly on the top quark mass. We used $M_t = 171.4 \pm 2.1$ GeV [8], and plotted the constraint corresponding to the central value (thick red/solid lines), as well as the boundaries of the 95% c.l. band (thinner red/solid lines). The contours are approximately independent of $\tan\beta$ for $3 \lesssim \tan\beta \lesssim 35$; the golden region shrinks rapidly outside of this range of $\tan\beta$. We use $\tan\beta = 10$ in the plots. The overlap between the regions of acceptably low fine-tuning (for definiteness, we choose $\Delta_t = 100$) and experimentally allowed Higgs mass defines the golden region, shaded in yellow in Figs. 2.

LEP2 searches for direct production of charginos and stops constrain both μ and $\tilde{m}_1$ to be above ≈ 100 GeV, and are largely independent of the rest of the MSSM parameters. The Tevatron stop searches yield a similar (though more model-dependent) bound on $\tilde{m}_1$.

In the presence of a large A_t term, stop and sbottom loops may induce a significant correction to the ρ parameter. For our purposes, it suffices to use the one-loop result. Using the PDG value $\rho = 1.0002^{+0.0004}_{-0.0007}$ [4], we obtain the 95% c.l. contours in the stop mass plane shown by the blue/dotted lines in Figs. 2. This constraint eliminates a part of the parameter space with very low $\tilde{m}_1$ and large δm.

The supersymmetric contribution to $g_\mu - 2$ depends sensitively on the slepton and weak gaugino mass scales, and only weakly on the parameters defining the golden region. We can expect a large contribution to the $b \to s\gamma$ rate from the $\tilde{t} - \tilde{H}$ loop. It is well known, however, that this can be cancelled by the contribution of the top-charged Higgs loop. A simplified analysis of this constraint based on [9] shows that for *any* values of the stop masses inside the golden region, and for any value of μ between 100 and 500 GeV, one can find values of m_A in the 100-1000 GeV range for which this cancellation ensures consistency with experiment.

2 The expected LHC signature

The golden region has the following interesting qualitative features:

- Both stops typically have masses below 1 TeV;
- A substantial mass splitting between the two stops: typically, $\delta m \gtrsim 200$ GeV;
- The stop mixing angle must be non-zero

The first feature implies that both $\tilde{t}_1$ and $\tilde{t}_2$ will be produced with sizeable cross sections at the LHC. The second feature implies that the decay mode $\tilde{t}_2 \to \tilde{t}_1 Z$ is kinematically allowed. The last feature guarantees that the vertex is non-zero, and the decay $\tilde{t}_2 \to \tilde{t}_1 Z$ indeed occurs.

The branching ratio of the $\tilde{t}_2 \to \tilde{t}_1 Z$ mode depends on which competing $\tilde{t}_2$ decay channels are available. The possible two-body channels are

$$t\tilde{g},\ t\tilde{\chi^0},\ b\tilde{\chi^+},\ \tilde{b}W^+,\ \tilde{b}H^+,\ \tilde{t}_1 h^0,\ \tilde{t}_1 H^0,\ \tilde{t}_1 A^0, \quad (5)$$

where $\tilde{\chi^0}$ and $\tilde{\chi^+}$ denote all neutralinos and charginos that are kinematically accessible, and flavor-changing couplings are assumed to be negligible.

For a more detailed analysis, we choose a benchmark point (BP) representative of the golden region (see Table 1). The physical stop masses are $\tilde{m}_1 = 400$ GeV and $\tilde{m}_2 = 700$ GeV, with maximal mixing $\theta_t = \pi/4$. Using `SuSpect`[6], we checked that the Higgs mass, the $b \to s\gamma$ branching ratio, the ρ parameter and the supersymmetric contribution to the muon anomalous magnetic moment at the BP are consistent with the current experimental constraints. The $\tilde{t}_2 \to \tilde{t}_1 Z$ mode has a substantial branching ratio, about 31%.

At the benchmark point, we find $\sigma(pp \to \tilde{t}_2 \tilde{t}_2^*) = 0.05$ pb. In about 52% of the events, either one or both of the produced stops decays in the $\tilde{t}_1 Z$ mode. This decay is followed by a cascade

$$\tilde{t}_1 \to \chi_1^+ b, \quad \chi_1^+ \to u\bar{d}\chi_1^0 \ / \ c\bar{s}\chi_1^0 \ / \ \ell^+\nu\chi_1^0, \quad (6)$$

where the jets and leptons are very soft due to a small chargino-neutralino mass splitting.

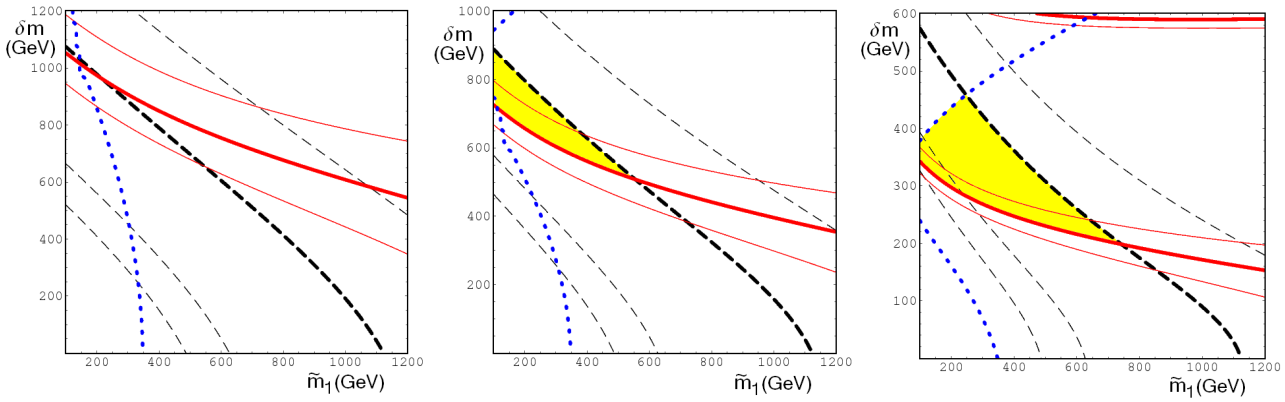

Fig. 2. Fine-tuning (black/dashed contours), Higgs mass bound (red/solid contours), and ρ-parameter (blue/dotted contours) constraints in the $(\tilde{m}_1,\, \delta m)$ plane. The three panels correspond to: $\theta_t = \pi/25, \pi/15, \pi/4$. In all panels $\tan\beta = 10$. The yellow/shaded intersection of the regions allowed by the three constraints is the MSSM "golden" region.

Table 1. The benchmark point: MSSM parameters, defined at the weak scale (dimensionful parameters in GeV).

m_{Q^3}	m_{u^3}	m_{d^3}	A_t	μ	m_A	$\tan\beta$	M_1	M_2	M_3	$m_{\tilde{q}}$	$m_{\tilde{\ell}}$
548.7	547.3	1000	1019	250	200	10	1000	1000	1000	1000	1000

Both the $\tilde{t}_1$ and $\tilde{t}_2$ decays always produce a b quark, as well as (assuming conserved R parity and a weakly interacting lightest supersymmetric particle) large missing transverse energy. In order to make the analysis as model-independent as possible, we therefore focus on an inclusive signature,

$$Z(\ell^+,\ell^-) + 2j_b + \not{E}_T + X, \qquad (7)$$

where $Z(\ell^+,\ell^-)$ denotes a lepton pair ($\ell = e$ or μ) with the invariant mass at the Z peak. The presence of energetic leptons ensures that essentially all such events will be triggered on.

To assess the observability of the signature (7), we have simulated statistically significant event samples for the signal and the most relevant SM backgrounds using the `MadGraph/ MadEvent v4` software package [10], which includes `Pythia` [11] and PGS.

The irreducible SM backgrounds that were analyzed in detail are $jjZZ$, $t\bar{t}Z$ and $t\bar{t}$, all of which can genuinely produce the signature (7). To isolate the signal events, we imposed the following set of cuts:

1. Two opposite-charge same-flavor leptons with $\sqrt{s(\ell^+\ell^-)} = M_Z \pm 2$ GeV.
2. Two hard jets with $p_T > 125$ GeV for the first and $p_T > 50$ GeV for the second;
3. At least one of the two highest-p_T jets must be b-tagged;
4. The boost factor of the reconstructed Z boson, $\gamma(Z) = 1/\sqrt{1-v_Z^2}$, must be larger than 2.0;
5. A missing E_T cut: $\not{E}_T > 225$ GeV.

The background production cross sections at the LHC and the efficiencies of these cuts are given in Table 2.

Assuming that the search is statistics-limited, we estimate that a 3-sigma observation would require 75 fb^{-1} of data, while a definitive 5-sigma discovery is possible with 210 fb^{-1}. Note that the $t\bar{t}$ background can be effectively measured from data by measuring the event rates with dilepton invariant masses away from the Z peak and performing shoulder subtraction.

We also considered several other irreducible SM backgrounds which are expected to be less significant, but might nevertheless be relevant. The most important one is $t\bar{t}j$, where j is a hard jet. The cross section for this channel is suppressed compared to $t\bar{t}$, but the presence of the additional hard jet increases the probability that the events will pass the jet p_T cut (cut 2). We find a parton-level cross section $\sigma(t\bar{t}j, p_T^j > 125\text{ GeV}) = 65$ pb. Assuming conservatively that all these events pass cut 2 and that the efficiencies of all other cuts are the same as for the $t\bar{t}$ sample, we expect that this background would add at most about 50% to the $t\bar{t}$ rate. As in the $t\bar{t}$ case, this contribution can be subtracted using data away from the Z peak in the lepton invariant mass distribution. Assuming that the statistical error dominates this subtraction, the net effect would be an increase in the integrated luminosity required to achieve the same level of significance by at most about 10%.

Other backgrounds we considered are three vector boson channels ZZZ, ZZW, and ZWW; as well as channels with single top production, tZj and $\bar{t}Zj$. Combining the parton-level cross sections for these channels with the branching ratios of decays producing the signature (7) results in event rates that are too small to affect the search.

While the SM processes considered above genuinely produce the signature (7), other SM processes may contribute to the background due to detector imperfections. We expect that the dominant among these is the process jjZ, with $Z \to \ell^+\ell^-$ and apparent $\not{E}_T$ due to jet energy mismeasurement or other instrumental issues. We conducted a preliminary investigation of

Table 2. Observability of the golden region signature (7). First row: Production cross sections at the LHC. Second row: Number of Monte Carlo events. Rows 3–8: Cut efficiencies, in%. Last row: Expected number of events for 100 fb^{-1}.

	signal: $\tilde{t}_2\tilde{t}_2^*$	$jjZZ$	$t\bar{t}Z$	$t\bar{t}$	jjZ
$\sigma_{\rm prod}$(pb)	0.051	0.888	0.616	552	824
total simulated	9964	159672	119395	3745930	1397940
1. leptonic Z(s)	1.4	4.5	2.6	0.04	2.1
2(a). $p_t(j_1) > 125$ GeV	89	67	55	21	41
2(b). $p_t(j_2) > 50$ GeV	94	93	92	76	84
3. b-tag	64	8	44	57	5
4. $\gamma(Z) > 2.0$	89	66	69	26	68
5. $\not\!\!E_T > 225$ GeV	48	2.2	4.4	1.7	< 0.9 (95% c.l.); 0 (ext.)
$N_{\rm exp}(100\ fb^{-1})$	16.4	2.8	10.8	8.8	< 177 (95% c.l.); 0 (ext.)

this background by generating and analyzing a sample of 1.4×10^6 jjZ events with $p_{T,\rm jet}^{\rm min} = 50$ GeV (see the last column of Table 2). None of the events in this sample pass the cuts 1-5. This allows us to put a 95% c.l. bound on the combined efficiency of this set of cuts for the jjZ sample of about 2×10^{-6}, corresponding to a background rate about 10 times larger than the signal rate. However, we expect that the actual jjZ background rate is well below this bound, since all 349 events in our sample that pass the cuts 1–4 in fact have $\not\!\!E_T$ below 50 GeV. We find that the $\not\!\!E_T$ distribution of these 349 events can be fit with an exponential, $N \propto e^{-0.10\not\!\!E_T}$, where $\not\!\!E_T$ is in units of GeV. Assuming that this scaling adequately describes the tail of the distribution at large $\not\!\!E_T$, we estimate that the rate of jjZ events passing all 5 cuts is completely negligible and that this background should not present a problem.

This conclusion is of course rather preliminary, and this issue should be revisited once the performance of the LHC detectors is understood using real data. Note that the necessity to understand the shape and normalization of the large apparent $\not\!\!E_T$ tail from SM processes with large cross sections is not unique to the signature discussed here, but is in fact crucial for most SUSY searches at the LHC.

3 Conclusions

Our analysis indicates that at the BP the signature (7) can be discovered at the LHC. The chosen BP is typical of the golden region, and this conclusion should generally hold as the MSSM parameters are varied away from the BP. There are, however, several exceptional parts of the parameter space where the observability of this signature could be substantially degraded:

- Large $\tilde{m}_2$ region: The $\tilde{t}_2$ production cross section drops rapidly with its mass;
- Small θ_t region: The branching ratio $\mathrm{Br}(\tilde{t}_2 \to Z\tilde{t}_1)$ is proportional to $\sin^2 2\theta_t$;
- Small $\tilde{t}_1$-LSP mass difference: The absence of hard jets in this case would make the signal/background discrimination more difficult.

Unfortunately, a positive identification of non-SM physics in this channel would *not* necessarily imply that the stops are split, since other MSSM processes may produce the same signature: for example, Z's can be produced in neutralino or chargino cascade decays. Careful comparisons of the rates with and without b jets, as well as the distribution of events in vector boson-jet invariant masses, can remove the ambiguity as explained in [1]. This may however take considerably more data than the discovery of an excess over the SM backgrounds in these channels.

Given the strong theoretical motivation for the signature discussed here, we encourage experimental collaborations to perform a more detailed study of its observability. If the first round of the LHC results points towards an MSSM-like theory, obtaining experimental information about the stop spectrum, and in particular testing whether the "golden region MSSM" hypothesis is correct, will become an important priority for the LHC experiments.

References

1. M. Perelstein and C. Spethmann, JHEP **0704**, 070 (2007) [arXiv:hep-ph/0702038].
2. R. Barbieri and G. F. Giudice, Nucl. Phys. B **306**, 63 (1988).
3. S. Schael *et al.* [ALEPH Collaboration], Eur. Phys. J. C **47**, 547 (2006)
4. W. M. Yao *et al.* [Particle Data Group], J. Phys. G **33**, 1 (2006).
5. G. Degrassi, S. Heinemeyer, W. Hollik, P. Slavich and G. Weiglein, Eur. Phys. J. C **28**, 133 (2003)
6. A. Djouadi, J. L. Kneur and G. Moultaka, arXiv:hep-ph/0211331.
7. M. Carena, J. R. Espinosa, M. Quiros and C. E. M. Wagner, Phys. Lett. B **355**, 209 (1995)
8. E. Brubaker *et al.* [Tevatron Electroweak Working Group], arXiv:hep-ex/0608032.
9. R. Barbieri and G. F. Giudice, Phys. Lett. B **309**, 86 (1993)
10. F. Maltoni and T. Stelzer, JHEP **0302**, 027 (2003).
11. T. Sjöstrand *et al.*, Comput. Phys. Commun. **135**, 238 (2001); T. Sjostrand, S. Mrenna and P. Skands, JHEP **0605**, 026 (2006)
12. L. T. Wang and I. Yavin, arXiv:hep-ph/0605296.